A NOVEL MICROFLUIDIC MIXER UTILIZING ELECTROKINETIC DRIVING FORCES UNDER LOW SWITCHING FREQUENCY

Lung-Ming Fu*, Che-Hsin Lin** and Chia-Yen Lee***

*Graduate Institute of Materials Engineering,
National Pingtung University of Science and Technology, Pingtung, Taiwan
**Department of Mechanical and Electro-mechanical Engineering,
National Sun Yat-Sen University, Kaohsiung, Taiwan
***Department of Mechanical and Automation Engineering, Da-Yeh University, Taiwan

loudyfu@mail.npust.edu.tw, chehsin@mail.nysu.edu.tw and cy@mail.dyu.edu.tw

Abstract : This paper presents a novel technique in which low-frequency periodic electrokinetic driving forces are utilized to mix electrolytic fluid samples rapidly and efficiently in a double-T-form microfluidic mixer. Without using any additional equipment to induce flow perturbations,only a single high voltage power source is required for simultaneously driving and mixing the sample fluids which results in a simple and low-cost system for the mixing purpose. The effectiveness of the mixer as a function of the applied electric field and the periodic switching frequency is characterized by the intensity distribution calculated downstream from the mixing zone. The present numerical and experimental results confirm that the proposed double-T-form micromixer has excellent mixing capabilities. The mixing efficiency can be as high as 95% within a mixing length of 1000 μm downstream from the secondary T-junction when a 100 V/cm driving electric field strength and a 2 Hz periodic switching frequency are applied. The results reveal that the optimal switching frequency depends upon the magnitude of the main applied electrical field. The rapid double-T-form microfluidic mixer using the periodic driving voltage switching model proposed in this study has considerable potential for use in Lab-on-a-Chip systems.

Introduction

Microfluidic chips designed for biochemical analysis applications have attracted considerable attention in the past decade. Using micromachining technology, a network of microchannels can be fabricated on a single quartz, glass, or plastic (PMMA, PDMS, PC) substrate to form a microchip capable of performing multiple procedures, e.g. sample handling, mixing, pretreatment, chemical reaction, separation, etc [1]. Bio-MEMS (Micro-Electric-Mechanical-System) devices are frequently required to conduct some form of biochemical reaction, and hence it is highly important that these devices have an effective mixing capability. However, implementing this capability is hindered by the very small scale of these microfluidic chips (typically in the range of several-ten micrometer), which tends to restrict the microchannel flows to the laminar flow regime and hinders the use of conventional mixing mechanisms. Microfluidic devices requiring a mixing operation have typically relied upon diffusive mixing achieved by bringing together the fluid streams to be mixed within a single channel [2]. However, diffusive mixing is slow and therefore requires the use of a long mixing channel if the fluid streams are to be completely mixed. Although this approach is acceptable for devices restricted to low flow rates, the length of the mixing channel required by devices operating with higher flow rates or with low analyte diffusion coefficients becomes prohibitively long.

Microfluidic devices which provide a more rapid mixing performance can be categorized in terms of the mixing methods they apply, namely active or passive. Active microfluidic mixers are particularly suitable for chamber mixing. The majority of active micromixers enhance mixing by stirring the flow streams using mechanical [3], magneto-hydrodynamic [4], electro-hydrodynamic [5], or acoustic streaming [6] techniques to create secondary flows. These secondary flows stretch and fold the material lines, hence reducing the diffusion path between the fluid streams and thereby promoting the diffusive mixing effect. However, the fabrication techniques for most active microfluidic mixers are complex and operation of these devices demands the provision of an external power source. Some other methods for mixing microfluidic samples actively were presented in the published literature [7]. For example, Lee *et al* [7] applied dielectrophoretic forces (in fluids with particles) to induced chaotic mixing effect in microchannel. Yang *et al* [8] reported an active micromixer using a lead-zirconate-titanate (PZT)-generated ultrasonic vibration to enhance mixing performance. Glasgow *et al* [9] presented a simply hydrodynamic pumping micromixer utilizing time-pulse flows to obtain good mixing efficiencies.Accordingly, many passive microfluidic mixers have been developed and investigated .

ISSN: 1727-1983

Formulation and numerical method

Numerical simulation of the present problem requires the solution of the electrical potential, ionic concentration, pressure, velocity components, and sample concentration throughout the computational domain. The current numerical solutions are based on the assumption of two-dimensionality (i.e. in the plane of the chip). It is noted that this assumption has been commonly employed in previous modeling of similar processes [10]. Furthermore, it is assumed that the dependent variables do not exhibit significant gradients in the thickness dimension (i.e. in the z-direction). Through the use of both two- and three-dimensional models, Patankar [10] showed this assumption to be reasonable in electroosmotic flows within microchannels of similar geometries to those considered in the present study. The main problem considered in this paper is the prediction of the electroosmotic flow in the double-T-form mixer under different operation modes. When an electric field is applied to a microchannel, the transient process of establishing electroosmotic flow has a duration of no more than a few hundred microseconds and is dependent on the microchannel dimensions and on the ionic concentrations of the buffer [11]. Since this duration is typically much shorter than the related characteristic times for injecting, separating, or mixing, etc, it can be neglected. Furthermore, thermal effects can also be neglected since the dissipation capability of a microfluidic chip is sufficiently high that no joule heating effect is observed for electrical fields of up to 800 V/cm [12].

Regarding the numerical simulation of electroosmotic flows, the current authors have previously developed physical models based on (a) the Poisson equation for the electrical potential and zeta potential, (b) the Nernst—Planck equations for the ionic concentration, (c) the full Navier—Stokes equations modified to include the effects of the body force due to the electrical and charge densities and (d) a concentration equation for the sample plug distribution. The detailed expressions of the governing equation, the initial conditions, and the boundary conditions are provided in reference [13].

$$\nabla^2 \psi = -\frac{\kappa^2}{2}\rho_e \tag{1}$$

$$\frac{\partial n_i}{\partial t} + \vec{u}\nabla n_i = \frac{1}{Sc\,\mathrm{Re}}\nabla^2 n_i + \frac{1}{Sc\,\mathrm{Re}}\left[\nabla\left(n_i \nabla \psi\right)\right] \tag{2}$$

$$\nabla \cdot \vec{u} = 0 \tag{3}$$

$$\frac{\partial \vec{u}}{\partial t} + \vec{u} \cdot \nabla \vec{u} = -\nabla p + \frac{1}{\mathrm{Re}}\nabla^2 \vec{u} - G_x \rho_e \nabla \psi \tag{4}$$

$$\frac{\partial C}{\partial t} + \vec{u} \cdot \nabla C = \frac{1}{Sc\,\mathrm{Re}}\nabla^2 C \tag{5}$$

Material and method

Chip Fabrication. The microfluidic chip was fabricated on low-cost microscope slides (25 x 75 x 1 mm, Mareinfeld, Germany) using a simple and reliable fabrication process proposed in our previous work. [13] The entire fabrication process lasted no longer than 10 hours. In addition, the silano-rich functional groups on glass surface make the liquid samples to be easily driven electrokinetically. A SEM image of close-up view and illustration of the proposed microfluidic mixer after fabrication is presented in Figure 1. The wings of the completed fabricated microfluidic device measured 1 cm in length, while the main mixing channel length was 4 cm. The widths of the wing and mixing channels were 80 and 100 μm, respectively. The measured depth for all the channels was 30 μm. Note that the upstream wings and downstream wings were 100 μm away from each other.

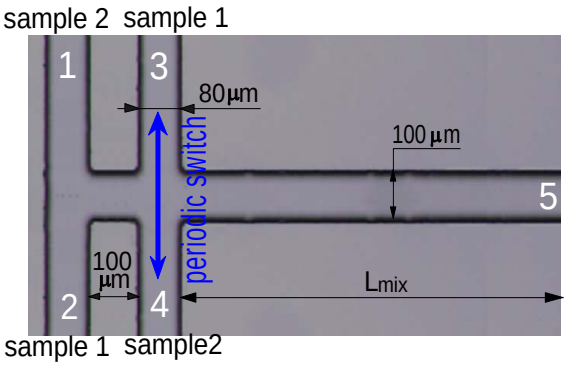

Figure 1: OM image of the close-up view and illustration of proposed double-T-form microfluidic mixer.

Experimental Setup. The two liquid samples used for the experimental tests were in the form of a 1 mM sodium borate buffer (pH=9.2) and a sodium borate buffer with 10^{-4} M Rhodamine B fluorescence dye, respectively. The samples were driven using only one programmable high-voltage power supply (MP-3500, Major Science, Taiwan) which is capable of high-speed switching of up to 10 Hz. No additional external power source was required for the mixing purpose. The experimental tests were performed under a fluorescence microscope (E-400, Nikon, Japan) equipped with a high resolution CCD camera (DXC-190, Sony, Japan) for images acquisition. The acquired optical images were than stored in a personal computer via a high speed DAQ interface (DVD PKB, V-gear, Taiwan).

Results and discussion

Parallel flow. Figure 2 presents the simulated electrical potential distributions and flow streamlines for two types of parallel flow conditions of *cis*-injection and *trans*-injection modes. Figure 2(a) shows the electrical potential distribution in the double-T-form microfluidic mixer for the Type A parallel flow, in which Sample 1 is injected though reservoirs 1 and 3, and Sample 2 is injected through reservoirs 2 and 4. An electric field of 100 V/cm is applied to each of the four reservoirs, while reservoir 5 is grounded. Figures 2(b) and 2(c) present the corresponding flow streamlines for these two injection types, respectively.

ISSN: 1727-1983

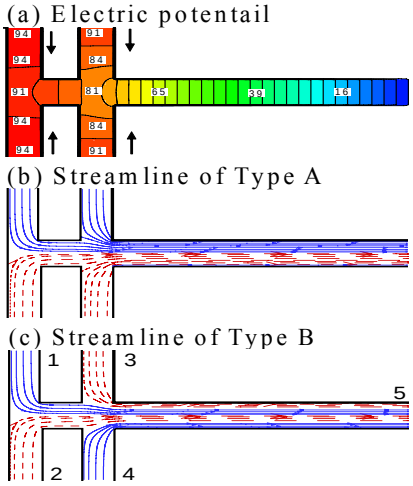

Figure 2: Numerical simulation results for: (a) electrical potential distributions, (b) Type A (*cis*-injection) streamlines, and (c) Type B (*trans*-injection) streamlines.

Figure 3 presents the numerical and experimental results for the species concentration distributions under the applied electric field of 100 V/cm. It is clear that the Type A parallel flow fails to provide an effective species mixing and that diffusion represents the dominant mixing mechanism. The mixing results shown in Figures 3(a) closely resemble those achieved in a conventional T-shaped micromixer. To quantify the degree of mixing within the mixing channel, the present study adopts the following mixing efficiency parameter [14]:

$$\sigma = \left(1 - \frac{\int_0^W |C - C_\infty| dy}{\int_0^W |C_o - C_\infty| dy}\right) \times 100\% \qquad (6)$$

where C is the species concentration profile across the width of the mixing channel, and C_o and C_∞ are the species concentrations in the completely unmixed (0 or 1) and completely mixed states (0.5), respectively.
The mixing efficiency results presented in Figure 4 indicate that the mixing efficiency of the Type A parallel flow is less than 41% at the end of the mixing channel (L_{mix} = 2500 μm).

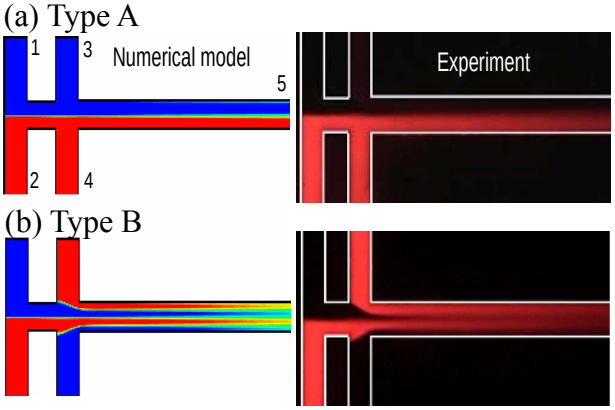

Figure 3: Numerical and experimental results for flow contours in parallel flows (a) Type A (*cis*-injection), and (b) Type B (*trans*-injection).

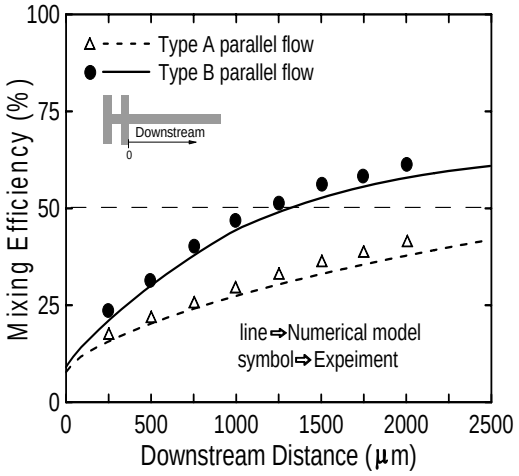

Figure 4: Mixing efficiency at different Types in parallel flow model

.

Figures 3(b) illustrate the species concentration distributions for the Type B parallel flow, in which Sample 1 is injected through reservoirs 1 and 4, and Sample 2 is injected through reservoirs 2 and 3. As shown in Figure 2(c), this injection arrangement increases the number of parallel flow streams in the mixing channel from two (Figure 2(b)) to four. The corresponding species concentration distribution results presented in Figure 3(b) clearly demonstrate that the contact area of the two samples is increased in Type B parallel flow. Hence, as shown in Figure 4, the mixing performance is increased from 41% (Type A) to 65% (Type B) at the end of the mixing section.

Periodic driving voltage switching mode. The mixing efficiency of microfluidic mixers can be enhanced by increasing the contact area and contact time of the different samples, creating irregular flow fields (such as separation bubbles) in the mixing channel, generating perturbations of the sample fluids, etc. However, fabricating microchannel configurations which generate irregular flow fields is challenging. Moreover, complex flow control mechanisms are required. Consequently, the present study adopts an interlaced sample injection mode controlled by a periodic switching method to increase the contact area and contact time of the two samples to be mixed and to generate perturbations of the fluid field.

In this operating mode, the driving voltages applied to reservoirs 1 and 2 are maintained at a constant value, while an equivalent driving voltage is switched periodically between reservoirs 3 and 4. Figure 5 presents the corresponding electrical potential distributions and streamlines for the two steps of this operating mode. In Figure 5(a) (Step 1), the voltages applied to reservoirs 1, 2 and 4 are established at an equivalent potential (or equivalent electric field) of 100 V/cm, while reservoir 3 is maintained in an open state (i.e. the electric field $\partial\phi/\partial y = 0$). Since there is no driving force in channel 3 (i.e. $\partial\phi/\partial y = 0$), the fluid remains motionless, as shown by the absence of streamlines in this channel in Figure 5(a). In Step 2 of this operating mode (Figure 5(b)), the driving voltage is switched from

ISSN: 1727-1983

reservoir 4 to reservoir 3. Hence, an equivalent driving force is generated in reservoirs 1,2 and 3, but the fluid remains motionless in channel 4. As shown in Figure 5, this periodic switching of the driving voltage between reservoirs 3 and 4 increases the flow perturbations and increases the contact area of the two samples.

Figure 6 presents the simulated and experimental species concentration distributions obtained when this switching mode is applied with a driving electric field of 100 V/cm and switching frequencies ranging from 1 Hz to 8 Hz (cases of 1, 2 and 8 Hz were selected). In this figure, Samples 1 and 2 are injected through channels 1 and 2, respectively, and establish a parallel flow between the two T-junctions. Meanwhile, a switching voltage is applied to channels 3 and 4 to inject Samples 2 and 1, respectively. This interlaced injection arrangement increases the flow perturbation and the contact area of the two samples within the mixing channel, and hence enhances the mixing performance. Figure 6(a) indicates that the species concentration distribution has a waveform pattern when the sample plugs are injected with a switching frequency of 1 Hz. The results of Figure 6(a) suggest that a switching frequency of 1 Hz generates sample plugs whose volumes are too large to be injected completely into the mixing channel. Consequently, the two samples fail to establish intimate contact in the mixing region. As shown in Figure 6(b), when the switching frequency is increased to 2 Hz, the contact area of the two samples is increased in the mixing channel. However, increasing the switching voltage beyond 2 Hz reduces the contact area since the amplitude of the concentration profile reduces (as shown in Figures 6(c)). When the switching frequency is increased to 8 Hz (Figure 6(c)), it can be seen that the species concentration has the form of parallel flow (see Figure 3(b)).

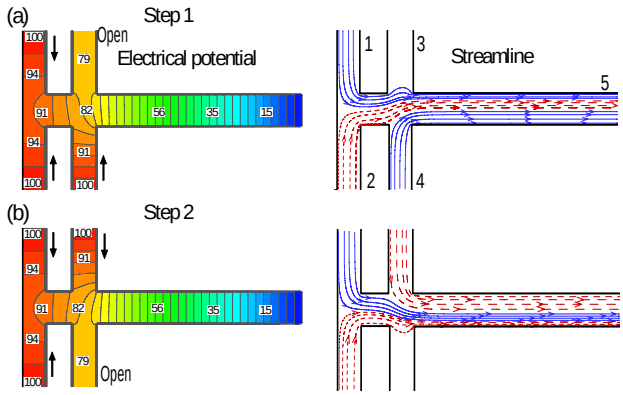

Figure 5: Electrical potential distributions and streamlines in two-step switching mode.

Figure 7 indicates the variation in the mixing efficiency along the mixing channel length (L_{mix} = 1200 μm) for a driving electric field of 100 V/cm and switching frequencies in the range of 0 Hz to 8 Hz. In the case of Type B parallel flow (0 Hz), mixing is achieved solely through the diffusion of the interlaced sample streams, and hence the maximum mixing efficiency only attains a value of 47.2%. At a switching frequency of 1 Hz, the mixing efficiency increases progressively along the mixing channel length and has a slightly undulating form. Meanwhile, at a switching frequency of 2 Hz, the mixing efficiency attains a maximum value of 95.3% at a distance of 1000 μm downstream from the secondary T-junction. Therefore, it is clear that the proposed periodic switching mode is capable of providing an effective and rapid mixing efficiency at this particular switching frequency. For switching frequencies of 4 Hz and 8 Hz, the mixing efficiencies obtained after a mixing length of 1200 μm are found to be 79.8% and 73.5%, respectively. As discussed previously, as the switching frequency is increased, the contact area and contact time of the two samples in the mixing channel are both reduced. Hence, the diffusion effect is lessened and the mixing efficiency diminished.

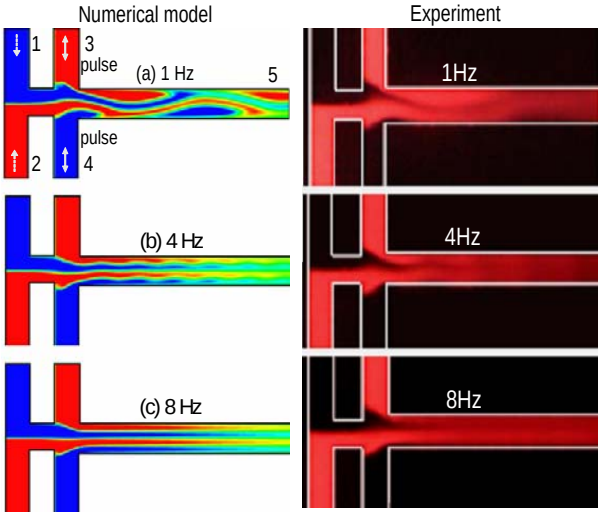

Figure 6: Species concentration distributions for switching frequencies of: (a) 1 Hz, (b) 2 Hz, and (c) 8 Hz for constant driving electric field of 100 V/cm through numerical and experimental analysis.

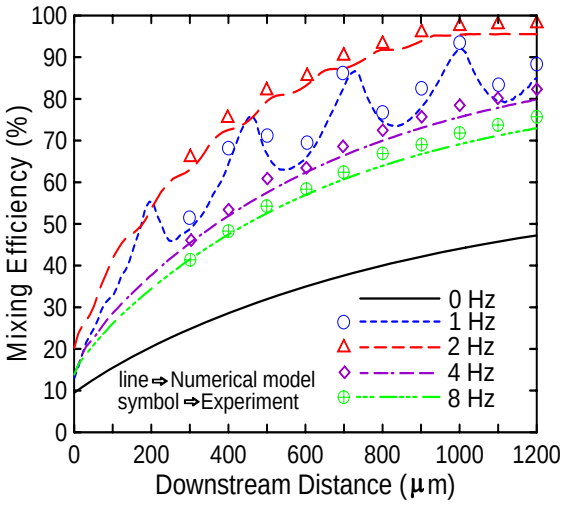

Figure 7: Comparison of mixing efficiency at different switching frequencies for constant driving electric field of 100 V/cm.

ISSN: 1727-1983

Influence of driving electric field strength. Figure 8 shows the simulated and experimental species concentration distributions obtained with various periodic switching frequencies and an increased driving electric field of 150 V/cm. Since a higher driving electric field increases the flow velocity, the contact time of the sample streams within the same channel length (1200 μm) is decreased compared to the previous cases (100 V/cm and 50 V/cm). Consequently, a longer mixing channel length and a higher periodic switching frequency must be employed if an equivalent mixing performance is to be attained.

Figure 9 indicates the variation in the mixing efficiency along the mixing channel length (L_{mix} = 2500 μm) for a driving electric field of 150 V/cm and switching frequencies in the range of 1 Hz to 8 Hz (cases of 1, 4 and 8 Hz were selected). The results show that a switching frequency of 4 Hz yields an optimal mixing efficiency of 96.2% at a mixing length of 1750 μm for an increased driving voltage of 150 V/cm. For switching frequencies of 1 Hz, 2 Hz and 8 Hz, the maximum mixing performance is obtained at the end of the mixing channel (L_{mix} = 2500 μm) and has a value of 86.2%, 92.1% and 85.3%, respectively. The results of Figure 9 indicate that when a higher driving electric field is applied, a longer mixing channel is required if an equivalent mixing performance is to be attained.

Figure 10 presents the optimal operating conditions for the current microfluidic mixer under different driving voltages and switching frequencies. It is noted that the average value of the mixing efficiency is calculated over the mixing channel region located between 1000 μm and 1200 μm downstream from the secondary T-junction. The results confirm that the mixing efficiency performance of all the current test cases can exceed 90%, hence demonstrating the feasibility of the proposed rapid microfluidic mixer.

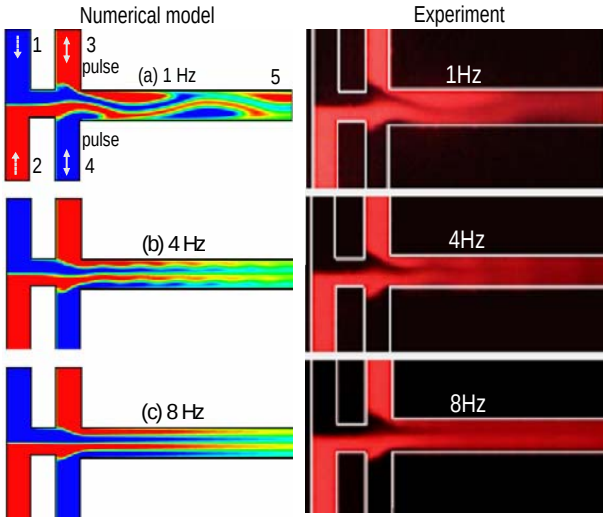

Figure 8: Species concentration distributions for switching frequencies of: (a) 1 Hz, (b) 4 Hz, and (c) 8 Hz for constant driving electric field of 150 V/cm through numerical and experimental analysis.

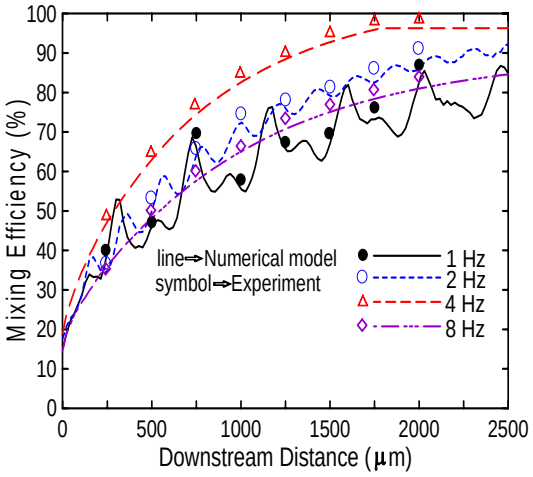

Figure 9: Comparison of mixing efficiency at different switching frequencies for constant driving electric field of 150 V/cm.

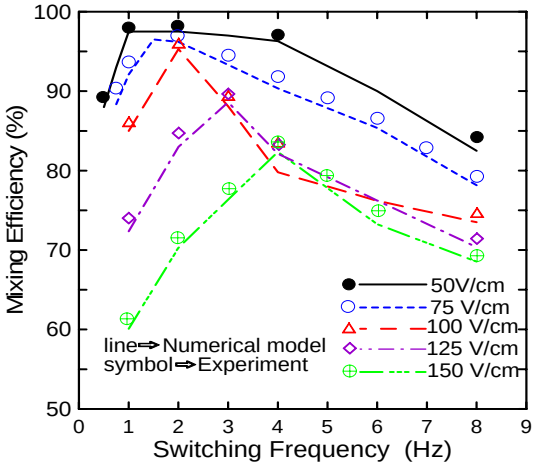

Figure 10: Numerical calculations and experimental evaluations of mixing efficiency for different driving electric fields and switching frequencies at cross section located 1200 μm downstream from the secondary T-junction.

Conclusions

This study has presented an active double-T-form microfluidic mixer utilizing a low-frequency switching electroosmotic flow. This double-T-form microfluidic mixer applies only one electrokinetic driving force which drives the sample fluids and produces periodic switching frequency simultaneously. It requires no other external driving force to induce perturbations to the flow field. Numerical and experimental show the mixing performance of microfluidic mixers can be enhanced by increasing the contact area and contact time of the sample streams, by creating irregular flow fields in the mixing channel, or by generating perturbations of the sample fluid, etc. This study has proposed a method in which interlaced injection samples, controlled electric field strengths, and periodic switching techniques have

ISSN: 1727-1983

been used in order to increase the contact area and contact time of the samples and to produce perturbations of the fluid field. The simulated and experimental results have shown that a mixing efficiency of 97% can be achieved within a mixing channel length of approximately 700 μm when a driving electric field strength of 50 V/cm is applied with a switching frequency of 1 Hz. When the driving electric field is increased to 150 V/cm, it has been shown that an equivalent mixing performance can only be achieved if a longer channel length and a higher switching frequency are applied. The optimized operating conditions of the proposed microfluidic mixer have been presented in terms of different driving electric field strengths and their corresponding switching frequencies. The results of the present study provide a valuable contribution to the ongoing development of micro-total-analysis systems.

Acknowledgment

The current authors gratefully acknowledge the financial support provided to this study by the National Science Council of Taiwan under Grant Nos. NSC 94-2320-B-020-001 and NSC 94-2320-B-110-003.

References

[1] HONG, J. W. and QUAKE S. R., (2002): 'Integrated nanoliter systems', *Nature Biotechnology*, **21**, pp. 1179-1183

[2] JACOBSON S. C., Mcknight T. E., RAMSEY J. M., (1999): 'Microfluidic Devices for Electrokinetically Driven Parallel and Serial Mixing', *Analytical Chemistry*, **71**, pp. 4455-4459

[3] LIU R. H., STREMLER M. A., SHARP K. V., OLSEN M. G., SANTIAGO J. G., ADRIAN R. J., AREF H. and BEEBE D. J., (2000): 'Passive mixing in a three-dimensional serpentine microchannel', *Journal of Microelectromechanical System,* **9**, pp. 190-197

[4]LEMOFF A. V., LEE A. P., (2000): 'An AC magnetohydrodynamic micropump', *Sensors and Actuators B*, **63**, pp. 178-185

[5] ODDY M. H., SANTIAGO J. G. and MIKKELSEN J. C., (2001): 'Electrokinetic instability micromixing', *Analytical Chemistry,* 73, pp. 5822-5832

[6]ZHU X., KIM E. S., (1998): 'Microfluidic motion generation with acoustic waves', *Sensors and Actuators A*, **66**, pp. 355-360

[7]DODGE A., JULLIEN M. C., LEE Y. K., NIU X., OKKELS F. and TABELING P., (2004): 'An example of a chaotic micromixer: the cross-channel micromixer', *Comptes Rendus Physique,* **5**, 559-563

[8]YANG Z., GOTO H., MATSUMOTO M. and MAEDA R., (2000): 'Active micromixer for microfluidic systems using lead-zirconate-titanate (PZT)-generated ultrasonic vibration', *Electrophoresis,* **21**, pp. 116-119

[9] GLASGOW I., AUBRY N., (2003): 'Enhancement of microfluidic mixing using time pulsing', *Lab on a Chip*, **3**, pp. 114-120

[10]PATANKAR N. A, Hu H. H., (1998): 'Numerical simulation of electroosmotic flow', *Analytical Chemistry*, **70**, pp. 1870-1881

[11] DOSE E. V., GUIOCHON G., (1993): 'Timescales of transient processes in capillary electrophoresis' *Journal of Chromatography A*, **652**, 263-275.

[12] JIN Y., LUO G. A., (2003): 'Numerical calculation of the electroosmotic flowat the cross region in microfluidic chips', *Electrophoresis*, **24**, pp. 1242–1252

[13] FU L. M., LIN C. H., (2003): 'Numerical analysis and experimental estimation of a low leakage injection technique for capillary electrophoresis', A*nalytical Chemistry*, **75**, pp. 5790-5796

[14] ERICKSON D., LI D., (2002): 'Influence of surface heterogeneity on electrokinetically driven microfluidic mixing', *Langmuir*, **18**, pp. 1883-1892

ISSN: 1727-1983